

## Reactive ion etching of organic polymers for application in waveguide trench molds

A. S. HOLLAND

*Australian Photonics CRC, School of Electrical & Computer Engineering, RMIT University, Melbourne 3001, Australia*

P. W. LEECH\*

*CSIRO Manufacturing and Infrastructure Technology, Clayton, Victoria, Australia*  
E-mail: Patrick.Leech@csiro.au

G. K. REEVES

*School of Electrical & Computer Engineering, RMIT University, Melbourne 3001, Australia*

Organic polymers have become important component materials in the development of optical waveguides [1, 2]. A critical requirement in the fabrication of rib waveguides in polymers has been the realization of suitable techniques of patterning and etching. The ion beam etching (IBE) of organic polymers to form rib waveguides [3–5] has been shown to produce excessive surface damage, thereby increasing the extent of optical scattering. Reactive ion etching (RIE) has also been used to fabricate rib structures [3, 5–10], which were directly etched into the core layer, typically to form a raised-rib (Fig. 1a). A patterned layer of resist was used to define the etch mask for the rib on the surface of the core layer. However, an inherent disadvantage of this configuration has been the tendency for dissolution of the solvent from the photoresist into the polymer, thereby necessitating a complex lithographic procedure [1, 3]. As an alternative configuration, the etching of the cladding layer to form a recessed mold for the rib (Fig. 1b) was advantageous since the cladding polymers were typically not dissolved in photoresist [1]. While the feasibility of forming inverted ribs using RIE has previously been established by Shi *et al.* [11], this report has included few details of the etching process. Based on results using oxygen gas, Dalton *et al.* [3] have suggested that RIE can be used for forming waveguides for conditions

corresponding to chemical etching, i.e., the ions in the system have such low kinetic energy that they do not cause pitting of the polymer surface. The aim of this letter has been to examine the reactive ion etching of UV curable polymers (Norland Optical Adhesive NOA61 and NOA73) and (Master Bond UV15). The polymers were selected as core layer materials (NOA61 and NOA73 with refractive index of 1.56 after curing) or as a cladding layer (UV15 with a refractive index of 1.48 after curing). The characteristics of the surfaces and profiles formed by reactive ion etching have been examined as a function of the etch parameters.

NOA61, NOA73, and UV15 were spin-coated onto wafers of polished silicon (76 mm). Before coating of the liquid photopolymer, the wafers were soaked in HF for 1 min to remove the native oxides. The samples were then cleaned by rinsing in acetone, followed by isopropanol, de-ionized water and blown dry in high purity nitrogen gas. This treatment was found to improve the wettability of the polymer films on the wafers. The liquid polymer was poured onto the center of the wafer and a spin speed of 500 rpm for 10 s was initially used to obtain a uniform dispersion across the surface. The speed was then ramped to 4000 rpm over 10 s and held for 30 s. Following spin-coating, the samples were immediately cured for 3 min using an unfiltered

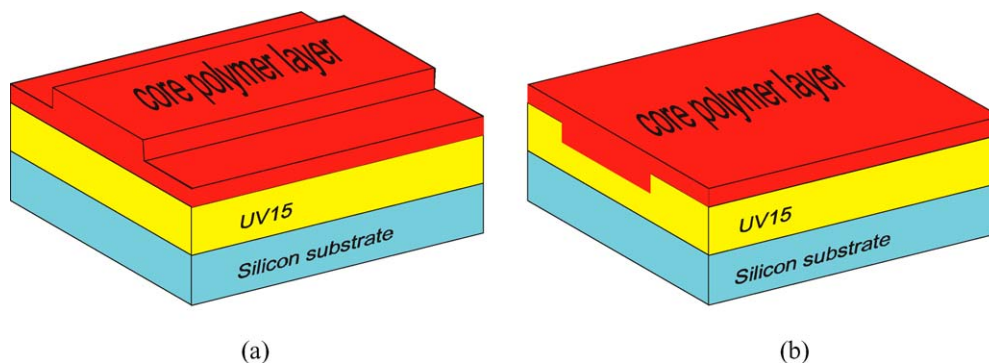


Figure 1 Schematic illustration of a (a) raised rib and (b) inverted rib waveguide.

\*Author to whom all correspondence should be addressed.

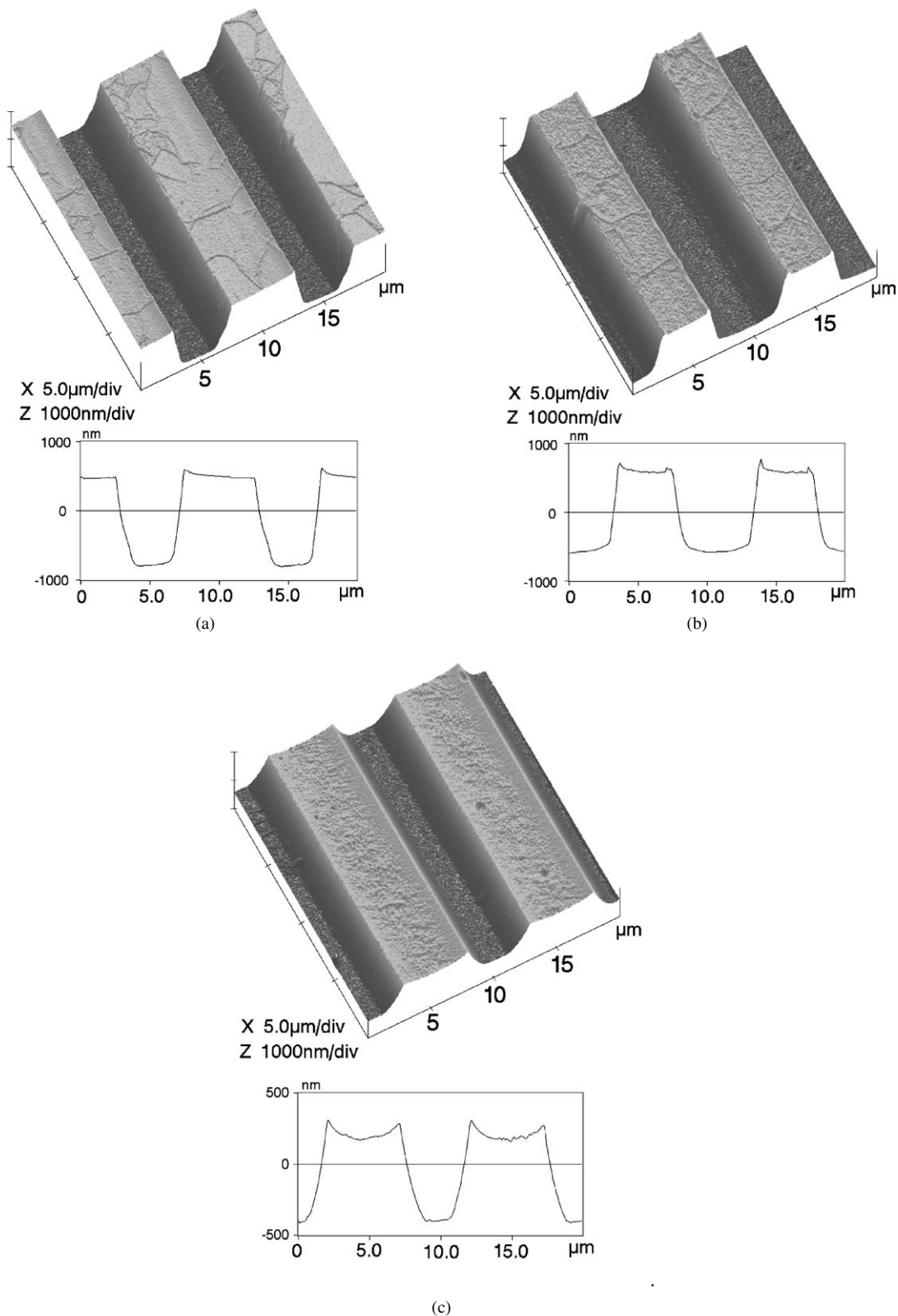


Figure 2 (a) AFM image and profile of a trench etched in NOA61 at 300 W in  $\text{CF}_4/\text{O}_2$  gases. The scale on the X and Y axes was  $5 \mu\text{m}/\text{division}$  and on the Z axis,  $1000 \text{ nm}/\text{division}$ . (b) AFM image and profile of a trench etched in NOA73 at 300 W in  $\text{CF}_4/\text{O}_2$  gases. The scale on the X and Y axes was  $5 \mu\text{m}/\text{division}$  and on the Z axis,  $1000 \text{ nm}/\text{division}$ . (c) AFM image and profile of a trench etched in UV15 at 300 W in  $\text{CF}_4/\text{O}_2$  gases. The scale on the X and Y axes was  $5 \mu\text{m}/\text{division}$  and on the Z axis,  $1000 \text{ nm}/\text{division}$ .

mercury lamp with intensity  $100 \text{ W}/\text{m}^2$  and then baked at  $120^\circ\text{C}$  for 30 min. The lamp produced UV wavelengths suitable for curing of the thermoset polymers. The subsequent baking step has been shown to further cure the thermoset polymer and increase the glass transition temperature,  $T_g$  [13]. Raising the value of  $T_g$  was

found advantageous in preventing the polymer from flowing and wrinkling during etching. The UV baking was also likely to decrease the sensitivity of the polymer surface to solvents [13]. After curing, the average surface roughness,  $R_a$ , of each polymer was determined by Atomic Force Microscope (AFM) as  $\leq 1 \text{ nm}$ . On the

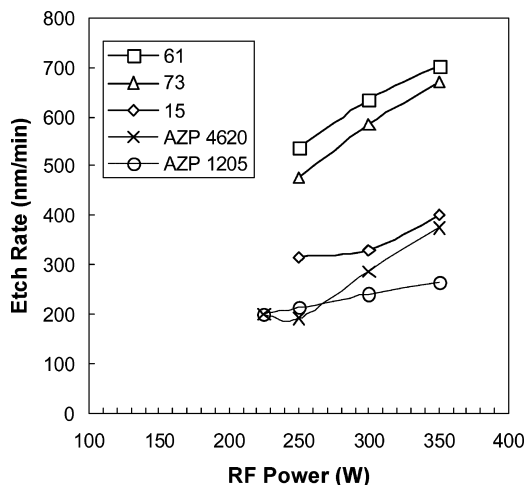


Figure 3 Etch rate versus rf power for NOA61, NOA73, UV15 polymers and resists.

surface of the polymer films, an array of waveguide patterns was formed in either Hoechst Celanese AZ 1512 resist or Hoechst Celanese AZ P4620 resist diluted by isopropyl alcohol in the ratio 1:1 to provide a mask during etching. The resist patterns were hard baked at 110 °C for 30 min.

The reactive ion etching was performed in a Surface Technology Systems STS320 system. The cathode in this system was 370 mm in diameter and was continuously cooled to a temperature of 20 °C. A base pressure in the chamber of  $\sim 1.33 \times 10^{-6}$  mbar was obtained by a turbomolecular pump backed by a rotary pump. The gas mixtures used were  $\text{CF}_4/\text{O}_2$  28 sccm/2 sccm and  $\text{CHF}_3/\text{O}_2$  28 sccm/2 sccm. The addition of fluorine containing gases to  $\text{O}_2$  has previously been found to increase the etch rate of organic materials [14]. The chamber pressure during etching was  $6.67 \times 10^{-2}$  mbar and etch times were 1–2 min. After etching, any residual resist was removed by immersion in Hoechst AZ 400 K (an aqueous alkaline developer). The etch depth, the average surface roughness,  $R_a$ , at the base of the etched trenches, and the slope of the side-walls were measured by AFM (Digital Instruments Dimension 3100).

AFM images of the patterns etched at 300 W in  $\text{CF}_4/\text{O}_2$  gases are shown in Fig. 2a to c. A greater depth of etch and verticality of the side-wall slope were clearly evident in the NOA61 and NOA73 polymers (Fig. 2a–b) than in UV15 (Fig. 2c). Measurements of the etch rates of the polymers are plotted as a function of rf power in Fig. 3. Also included in Fig. 3 were the etch rates for AZ 1512 and AZ P4620 resists after baking at 110 °C for 30 min. The etch rate increased more steeply with rf power for the NOA61 and NOA73 polymers than for UV15. At 350 W, the ratio of etch rates for the NOA61:NOA73:UV15 polymers in  $\text{CF}_4/\text{O}_2$  gases was  $\sim 700:670:400$  nm/min. In comparison, during etching in the  $\text{CHF}_3/\text{O}_2$  gases, the measured etch rates of the polymers (Table I) were lower by a factor of  $\sim 2$  than with the  $\text{CF}_4/\text{O}_2$  gases. The order of ranking of etch rates in  $\text{CHF}_3/\text{O}_2$  gases at 350 W was also NOA61:NOA73:UV15 with etch rate ratios of  $\sim 340:300:260$  nm/min. A feature of etching in the  $\text{CHF}_3/\text{O}_2$  gases was the greater etch rate ratio of

TABLE I Reactive ion etch rate of UV15, NOA61, and NOA73 polymers in  $\text{CHF}_3/\text{O}_2$  gases

Power (W)	Etch rate (nm/min)			
	AZ1500	UV15	NOA61	NOA73
250	25			
325	33.3			
350	30	263	338	242

the polymer to the resist (etch rate ratio of 8:1–10:1) than in  $\text{CF}_4/\text{O}_2$  gases (etch rate ratio of  $\sim 2:1$ ).

In Fig. 4, the values of  $R_a$  for the etched surfaces are plotted as a function of rf power which corresponded directly to an increase in ion energy. All three organic polymers have shown a significant increase in  $R_a$  with rf power, particularly above 300 W. The NOA61 and NOA73 polymers developed a similar value of  $R_a$  during etching at all power levels which was significantly greater than  $R_a$  obtained for UV15.

The side-wall angle of trenches etched by RIE in  $\text{CF}_4/\text{O}_2$  is plotted in Fig. 5 as a function of rf power. NOA61 and NOA73 polymers have both shown a similar decrease in side-wall angle ( $50\text{--}60^\circ$ ) with increasing power while UV15 formed trenches with a

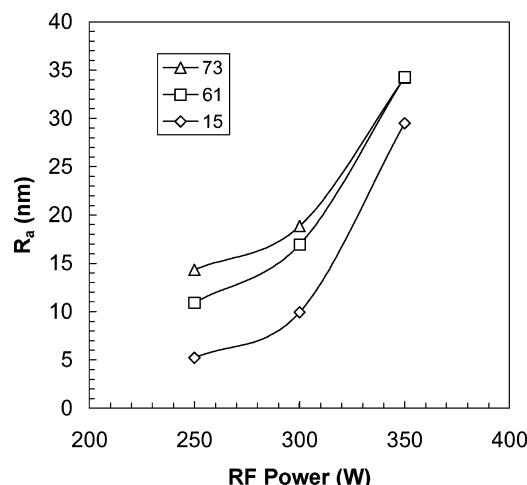


Figure 4  $R_a$  of the polymers versus rf power after etching in  $\text{CF}_4/\text{O}_2$  gases.

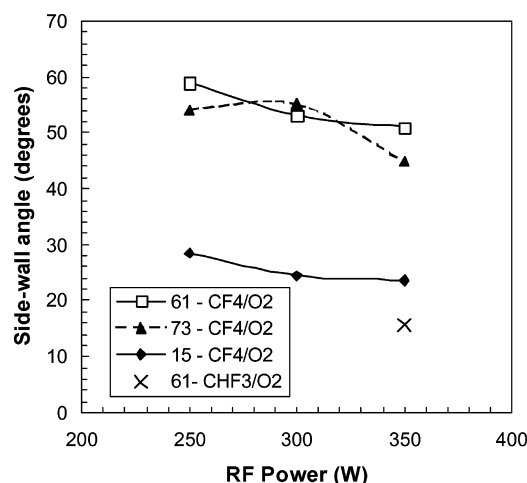


Figure 5 Side-wall angle versus rf power.

lower angle (20–30°). Trenches which were etched in CHF<sub>3</sub>/O<sub>2</sub> gases at 350 W have shown a reduced value of side-wall angle of ~14° (UV15), 16° (NOA61), and 13° (NOA73).

In summary, the NOA61 and NOA73 polymers have shown a greater etch rate (~600–700 nm/min) than UV15 (~400 nm/min) in CF<sub>4</sub>/O<sub>2</sub> gases and in CHF<sub>3</sub>/O<sub>2</sub> gases. The etch rate for the three polymers in the CF<sub>4</sub>/O<sub>2</sub> mixture was larger by a factor of ~2 than in CHF<sub>3</sub>/O<sub>2</sub> gases although the selectivity between polymer and resist mask was enhanced (etch rate ratio of 8:1–10:1) in CHF<sub>3</sub>/O<sub>2</sub>. The NOA61 and NOA73 polymers have shown a steeper verticality of the side-wall slope but a greater surface roughness, *R*<sub>a</sub>, at the base in etched trenches than in the UV15 polymer.

## References

1. W. H. STEIER, A. CHEN, S.-S. LEE, S. GARNER, H. ZHANG, V. CHUYANOV, L. DALTON, F. WANG, A. REN, C. ZHANG, G. TODOROVA, A. HARPER, H. FETTERMAN, D. CHEN, A. UDUPA, D. BHATTACHARYA and B. TSAP, *Chem. Phys.* **245** (1999) 487.
2. R. DE RIDDER, A. DRIESSEN, E. RIKKERS, P. LAMBECK and M. DIEMEER, *Opt. Mater.* **12** (1999) 205.
3. L. DALTON, A. HARPER, A. REN, F. WANG, G. TODOROVA, J. CHEN, C. ZHANG and M. LEE, *Ind. Eng. Chem. Res.* **38** (1999) 8.
4. A. HOLLAND, D. SIMON, H. MENDIS, A. MITCHELL, G. AMARASINGHE, R. SHANKS, S. HUNTINGTON and M. AUSTIN, in Proc. Polymer Processing Society PPS-19 Conference, Melbourne, July 2003.
5. S. GARNER, V. CHUYANOV, S.-S. LEE, A. CHEN, W. STEIER and L. DALTON, *IEEE Photon. Technol. Lett.* **11**(7) (1999) 842.
6. D. AN, Z. SHI, J. M. TABOADA, Q. ZHOU, X. LU and R. T. CHEN, *Appl. Phys. Letts.* **76**(15) (2000) 1972.
7. M. B. J. DIMEER, *Opt. Mater.* **9** (1998) 192.
8. C. ZHANG and L. DALTON, *Chem. Mater.* **13** (2001) 3043.
9. S.-W. AHN and S.-Y. SHIN, *Opti. Commun.* **197** (2001) 289.
10. M.-C. OH, H. ZHANG, C. ZHANG, H. ERLIG, Y. CHANG, B. TSAP, D. CHANG, A. SZEP, W. STEIER, H. FETTERMAN and L. DALTON, *IEEE J. Select. Top. Quant. Electr.* **7**(5) (2001) 826.
11. Y. SHI, W. LIN, D. OLSEN, J. BECHTEL, H. ZHANG, W. STEIER, C. ZHANG and L. DALTON, *Appl. Phys. Letts.* **77**(1) (2000).
12. A. CHEN, K. KAVIANI, A. REMPEL, S. KALLURI, W. STEIER, Y. SHI, Z. LIANG and L. DALTON, *J. Electrochem. Soc.* **143**(11) (1996) 3648.
13. Technical Data Sheet, Master Bond Polymer System UV15.
14. S. WOLF and R. N. TAUBER, "Silicon Processing for the VLSI Era Vol. 1 Process Technology" (Lattice Press, Sunset Beach, CA, 1987) p. 564.

Received 1 October 2003  
and accepted 12 January 2004